Publications

7-2020

Dynamics of Discontinuities in Elastic Solids

Arkadi Berezovski
Tallinn University of Technology, arkadi.berezovski@cs.ioc.ee

Mihhail Berezovski
Embry-Riddle Aeronautical University, berezovm@erau.edu

Dynamics of discontinuities in elastic solids

Arkadi Berezovski[1] and Mihhail Berezovski[2]

Abstract

Discontinuities in elastic solids are represented in the paper as singular sets of material points. Evolution of a discontinuity is driven by the configurational force acting at such a set. The main attention is paid to the determination of the velocity of a propagating discontinuity. Martensitic phase transition front and brittle crack are considered as representative examples.

Keywords

Driving forces, phase transition front, brittle crack, numerical methods, elastic solids

In memory of Professor Gérard A. Maugin

Introduction

In the framework of continuum mechanics, a discontinuity can be idealized as a surface of discontinuity in 3D and a line defect in 2D (Maugin (2000)). Among various possible discontinuities in elastic solids, propagating discontinuities hold a special place due to their theoretical complexity and practical importance. Dynamics of such discontinuities is determined by two factors, i.e., by the driving force acting at the discontinuity and by the discontinuity velocity. Both the driving force and the velocity of discontinuity have been subjects of intensive research in the case of phase transition fronts (Abeyaratne and Knowles (2006)) and crack dynamics (Freund (1990); Broberg (1999); Ravi-Chandar (2004)). The driving force acting at discontinuity is a specific

[1]Department of Cybernetics, School of Science, Tallinn University of Technology, Estonia
[2]Department of Mathematics, Embry-Riddle Aeronautical University, FL, USA

Corresponding author:
Arkadi Berezovski, Department of Cybernetics, School of Science, Tallinn University of Technology, 21 Akadeemia Rd, 12618, Tallinn, Estonia.
Email: arkadi.berezovski@cs.ioc.ee

example of the well established concept of configurational forces (Maugin (1995); Kienzler and Herrmann (2000); Gurtin (2000); Maugin (2011)). However, the velocity of a discontinuity cannot be uniquely determined in the standard continual framework. A possibility of the computation of the value of the velocity of a discontinuity is discussed in the paper on the basis of the thermodynamically consistent finite-volume algorithm (Berezovski et al. (2008)).

Discontinuities in elastic solids attracted the attention of Prof. Maugin for decades. His main contribution in this field was the advancement of the concept of driving (configurational) forces acting at a discontinuity. The formulation of the principle of virtual power for media presenting singular surfaces and interfaces (Daher and Maugin (1986)) can be considered as the starting point. At the next step, this formulation was applied for nonlinear electroelastic solids and extended on the case of shocks (Ani and Maugin (1988, 1989)). Various representations of the balance of linear momentum in nonlinear inhomogeneous elasticity were critically examined to demonstrate their similarity and distinction (Maugin and Trimarco (1992); Maugin (1993)).

The field theoretic formulation of nonlinear anistropic inhomogeneous elasticity capturing the essential material properties uses notions of pseudomomentum, Eshelby stress, and inhomogeneity force. This formalism has been applied to the case of an elastic body containing a crack of finite extent, following in the notion of suction force acting at the tip of the crack (Dascalu and Maugin (1993); Maugin (1993)). The J-integral and energy-release rates in dynamical fracture were analyzed in terms of material formulation for magnetoelastic (Maugin (1994)), electroelastic (Dascalu and Maugin (1994)), piezoelectric (Dascalu and Maugin (1995)), and ferromagnetic (Sabir and Maugin (1996)) finitely deformable materials with cracks.

Another example of the discontinuity is provided by phase-transition fronts in thermoelastic solids. The transition of a thermoelastic phase into another one with different symmetry is viewed as the progress of a material inhomogeneity (Maugin and Trimarco (1995a,b)). This progress is intimately related to the canonical formulation of balance laws, which determines the jump relations that must hold at a coherent phase-transition front. All these findings were summarized by unifying the notion of material force for all types of inhomogeneities in elastodynamics, fracture, defect mechanics, and in the propagation of phase transition fronts (Maugin (1995)). The developed formalism has been extended then on thermoelastic ferromagnets (Fomethe and Maugin (1997)), thermoelectroelastic crystals (Maugin and Trimarco (1997)), and hard ferromagnets (Fomethe and Maugin (1998)).

As a logical consequence, the canonical formalism that considers simultaneously the second law of thermodynamics and the balance of canonical momentum is used to incorporate the case of shock waves among those singularity sets whose dissipation is in fact related to the power expanded by a driving force in an irreversible motion of the singularity set (Maugin (1997, 1998)). It was shown that the formal expression of the driving force acting on a one- dimensional or two-dimensional singular set of material points (crack tip in fracture, phase-transition front or shock wave) and of the accompanying dissipation in an irreversible progress of the set is independent of

the precise material behavior at regular points (Maugin and Berezovski (1999); Maugin (2000); Maugin and Trimarco (2001)).

The material symmetry of the physical system is broken by the presence of a field singularity of a given dimensionality (point, line, surface, volume). Usually all these domains were studied separately but a general framework (Eshelbian mechanics) was developed in a somewhat synthetic form. In this framework, all configurational forces appear as forces of a non-Newtonian nature, acting on the material manifold (the set of points building up the material whether discrete or continuous) and not in physical space which remains the realm of Newtonian forces. That is, configurational forces acquire a true physical meaning only in so far as they contribute to the global dissipation (Maugin and Trimarco (2001); Maugin (2003)).

Configurational forces are thermodynamic conjugates to irreversible material body evolutions such as extension of cracks, progress of phase-transition fronts, movement of shock waves, etc. They do correspond to a change of material configuration. Various configurational forces such as those appearing in inhomogeneous bodies, at the tip of a propagating crack, at the surface of a propagating phase-transition front, or of a shock wave, and those due to local structural rearrangements (plasticity, damage, growth), were unified and examined from the point of view of their dissipated power (Maugin and Berezovski (2008); Maugin (2011)).

Theoretical elaboration was complemented by numerical simulation of moving discontinuities. It was provided in a series of papers devoted to stress-induced martensitic phase-transition front propagation (Berezovski and Maugin (2002); Berezovski et al. (2002, 2003); Berezovski and Maugin (2003, 2005c); Berezovski et al. (2006)). The results were summarized in the book by Berezovski et al. (2008).

While the configurational driving force acting at the phase boundary can be calculated by means of standard numerical methods, the velocity of the phase transition front or the crack tip depends on an unknown stress jump at the discontinuity. The problem cannot be resolved theoretically without an additional assumption regarding a kinetic law (Truskinovsky (1987); Abeyaratne and Knowles (1990); Maugin and Trimarco (1995b)). Fortunately, it has an algorithmic solution based on thermodynamic consistency (Maugin and Berezovski (2003); Berezovski and Maugin (2004)) in the case of singular surfaces (Berezovski and Maugin (2005a,b); Maugin and Berezovski (2009)). In what follows we describe the numerical algorithm in detail on example of martensitic phase-transition front propagation. A much more sophisticated consideration was proposed for the dynamics of straight-through brittle crack (Berezovski et al. (2007); Berezovski and Maugin (2007b, 2010)).

Martensitic phase-transition front

The most clear example of an evolving discontinuity in elastic solids is a stress-induced phase-transition front between martensite and austenite phases in a shape memory material, because its continuum description can be considered in one-dimensional setting (Abeyaratne and Knowles (2006)). Martensitic transformations are first order, diffusionless, shear solid state structural changes (Christian (1965)). The

propagation of phase interfaces in shape-memory alloys under applied stress is an experimentally observed phenomenon, which provides a hysteretic behaviour of shape-memory materials (Shaw and Kyriakides (1997)). At the continuum level of description, the phase-transition front is represented by a surface of discontinuity of zero thickness separating the different homogeneous austenite and martensite phases (Abeyaratne and Knowles (2006)).

The simplest formulation of the stress-induced phase-transition front propagation problem is given in the case of an isothermal uniaxial motion of a bar. Consider an isothermal motion of a bar with a unit cross-section. The bar occupies the interval $0 < x < L$ in a reference configuration and assumed to be long compared to its diameter so it is under uniaxial stress state and the stress $\sigma(x, t)$ depends only on the axial position and time. The density of the material ρ is assumed constant.

Let $u(x, t)$ be the displacement of a point x at time t in the reference configuration. Then strain and velocity fields are given by

$$\varepsilon(x,t) = \frac{\partial u}{\partial x}, \quad v(x,t) = \frac{\partial u}{\partial t}, \tag{1}$$

respectively. Away from a phase boundary, balance of linear momentum and kinematic compatibility require that

$$\rho \frac{\partial v}{\partial t} = \frac{\partial \sigma}{\partial x}, \tag{2}$$

$$\frac{\partial \varepsilon}{\partial t} = \frac{\partial v}{\partial x}, \tag{3}$$

where the function $\sigma(\varepsilon)$ specifies the stress-strain relation.

The velocity and strain fields subject to the following initial and boundary conditions:

$$\varepsilon(x,0) = v(x,0) = 0, \qquad \text{for} \quad 0 < x < L, \tag{4}$$

$$v(0,t) = v_0(t), \quad \varepsilon(L,t) = 0, \quad \text{for} \quad t > 0, \tag{5}$$

where $v_0(t)$ is a given time-dependent function.

Suppose now that an isolated strain discontinuity **S** propagates along the bar with a velocity V. On the discontinuity **S** the balance laws reduce to the Rankine-Hugoniot jump conditions

$$V[\![\varepsilon]\!] + [\![v]\!] = 0, \tag{6}$$

$$V[\![\rho v]\!] + [\![\sigma]\!] = 0, \tag{7}$$

where

$$[\![A]\!] = A^+ - A^- \tag{8}$$

denotes the jump of the enclosure at discontinuity, and $A^\pm$ denote the uniform limits of A in approaching the discontinuity from the $\pm$ side.

It is well understood that the martensitic phase transformation is a dissipative process that involves entropy change (Abeyaratne and Knowles (2006)). The strain discontinuity

that occurs across a propagating phase boundary is a source of dissipation. The energy dissipation at moving martensitic phase boundaries explains the experimentally observed hysteresis. Irreversibility due to the dissipation leads one to the notion of the driving force on a phase boundary (Heidug and Lehner (1985); Truskinovsky (1987); Abeyaratne and Knowles (1990); Maugin and Trimarco (1995b)). Therefore, jump relations (6), (7) must be supplemented by the entropy inequality in the form

$$f_{\mathbf{s}} V \geq 0. \tag{9}$$

where

$$f_{\mathbf{s}} = -[\![W]\!] + \langle \sigma \rangle [\![\varepsilon]\!], \tag{10}$$

is the associated configurational driving force, W is free energy per unit volume, $\langle \sigma \rangle = (\sigma^+ + \sigma^-)/2$.

The macroscopic jump conditions do not provide enough information to specify the velocity of the phase boundary V uniquely. The uniqueness of the solution is provided by the introduction of two supplementary constitutive-like relationships: a kinetic law for a driving force that establishes the speed of the transformation front and a nucleation criterion (Abeyaratne and Knowles (2006)). The constitutive theory of kinetic relations is not completely established yet. However, the velocity of the phase boundary can be determined algorithmically in spite of the absence any kinetic relation. The main idea is based on the relation

$$V^2 = \frac{[\![\sigma]\!]}{\rho [\![\varepsilon]\!]}, \tag{11}$$

which follows from jump relations (6) and (7) since the density ρ is constant in the considered case. The only question is in the accuracy of the determination of the stress (or strain) jump at the interface. Fortunately, the stress jump can be accurately determined algorithmically.

Finite volume interpretation

Averaged and excess quantities

Numerical methods deal with approximated values of field variables. In finite volume methods such an approximation is achieved by simple averaging over the computational cell. This means that the value of any extensive quantity A is the sum of its averaged counterpart $\bar{A}$ and its excess part A_{ex},

$$A = \bar{A} + A_{ex}. \tag{12}$$

In the case of elasticity

$$\sigma = \bar{\sigma} + \Sigma \qquad v = \bar{v} + \mathcal{V}. \tag{13}$$

Here overbars still denote averaged quantity and Σ and $\mathcal{V}$ are the corresponding excess quantities. However, the introduced excess quantities are useless (and even superfluous) until the rules of their treatment are specified.

Let us introduce a computational grid of cells $C_n = [x_n, x_{n+1}]$ with interfaces $x_n = n\Delta x$ and time levels $t_k = k\Delta t$. For simplicity, the grid size Δx and time step Δt are assumed to be constant.

Integrating the balance of linear momentum (1) over the computational cell gives:

$$\rho\frac{\partial}{\partial t}\int_{x_n}^{x_{n+1}} v dx = \sigma_n^+ - \sigma_n^- = \overline{\sigma}_n + \Sigma_n^+ - \overline{\sigma}_n - \Sigma_n^- = \Sigma_n^+ - \Sigma_n^-, \qquad (14)$$

where superscripts "+" and "-" denote values of the quantities at right and left boundaries of the cell, respectively. Similarly, the kinematic compatibility (2) leads to

$$\frac{\partial}{\partial t}\int_{x_n}^{x_{n+1}} \varepsilon dx = v_n^+ - v_n^- = \overline{v}_n + \mathcal{V}_n^+ - \overline{v}_n - \mathcal{V}_n^- = \mathcal{V}_n^+ - \mathcal{V}_n^-. \qquad (15)$$

The definition of averaged quantities

$$\overline{\rho v}_n = \frac{1}{\Delta x}\int_{x_n}^{x_{n+1}} \rho(x, t_k)v(x, t_k)dx, \quad \overline{\varepsilon}_n = \frac{1}{\Delta x}\int_{x_n}^{x_{n+1}} \varepsilon(x, t_k)dx, \qquad (16)$$

allows us rewrite a first-order Godunov-type scheme in terms of excess quantities

$$(\overline{\rho v})_n^{k+1} - (\overline{\rho v})_n^k = \frac{\Delta t}{\Delta x}\left(\Sigma_n^+ - \Sigma_n^-\right), \qquad (17)$$

$$\overline{\varepsilon}_n^{k+1} - \overline{\varepsilon}_n^k = \frac{\Delta t}{\Delta x}\left(\mathcal{V}_n^+ - \mathcal{V}_n^-\right). \qquad (18)$$

Here the superscript k denotes time step and the subscript n denotes the number of computational cell. Now we need to compute the values of excess quantities.

Excess quantities in the bulk

Though the excess quantities are determined formally everywhere inside computational cells, we need to know their values only at the boundaries of the cells, where they play the role of numerical fluxes. The boundaries between computational cells represent regular material points and therefore the total stress should be continuous across the boundary between cells

$$[\![\overline{\sigma} + \Sigma]\!] = 0. \qquad (19)$$

The same condition follows from the jump relation for the linear momentum, because the boundary between computational cells does not move. Jump relation (19) can be considered as the *continuity of genuine unknown field* at the boundaries between computational cells.

Similarly, the jump relation following from the kinematic compatibility reads

$$[\![\overline{v} + \mathcal{V}]\!] = 0. \qquad (20)$$

It is instructive to represent jump relations (19) and (20) in the numerical form

$$(\Sigma^+)_{n-1} - (\Sigma^-)_n = (\overline{\sigma})_n - (\overline{\sigma})_{n-1}, \qquad (21)$$

$$(V^+)_{n-1} - (V^-)_n = (\bar{v})_n - (\bar{v})_{n-1}. \tag{22}$$

The values of excess stresses and excess velocities at the boundaries between computational cells are not independent. Using the conservation of Riemann invariants we have for for excess quantities

$$\rho_n c_n \mathcal{V}_n^- + \Sigma_n^- \equiv 0, \tag{23}$$

$$\rho_{n-1} c_{n-1} \mathcal{V}_{n-1}^+ - \Sigma_{n-1}^+ \equiv 0, \tag{24}$$

It follows that we have the system of linear equations for the determination of excess quantities. This system of equations can be solved exactly for each boundary between computational cells. After that the field quantities can be updated for the next time step by means of numerical scheme (17)-(18).

Excess quantities at the phase boundary

To determine the values of excess stresses at the moving phase boundary, we keep the continuity of excess stresses across the phase boundary

$$[\![\Sigma]\!] = 0, \tag{25}$$

which yields

$$\left(\Sigma^+\right)_{p-1} - \left(\Sigma^-\right)_p = 0, \tag{26}$$

where phase boundary is placed between elements $(p-1)$ and (p).

The last jump relation can be interpreted as the *conservation of the genuine jump at the phase boundary* in the numerical calculations because (25) means that

$$[\![\sigma]\!] = [\![\bar{\sigma} + \Sigma]\!] = [\![\bar{\sigma}]\!]. \tag{27}$$

To be consistent, we require the conservation of the genuine jump also for velocity

$$[\![V]\!] = 0. \tag{28}$$

We still keep the relations between excess stresses and excess velocities (23), (24). This means that in terms of excess stresses Eq. (28) yields

$$\frac{(\Sigma^+)_{p-1}}{\rho_{p-1} c_{p-1}} + \frac{(\Sigma^-)_p}{\rho_p c_p} = 0. \tag{29}$$

It follows from the conditions (26) and (29) that the values of excess stresses vanish at the phase boundary

$$(\Sigma^+)_{p-1} = (\Sigma^-)_p = 0. \tag{30}$$

Similarly, due to relations (23), (24)

$$(V^+)_{p-1} = (V^-)_p = 0. \tag{31}$$

Now all the excess quantities at the phase boundary are determined, and we can update the state of the elements adjacent to the phase boundary.

Thus, the supplementary constitutive information needed to avoid the non-uniqueness of the solution of the boundary-value problem is provided by means of non-equilibrium jump relations at the moving phase boundary, which are formulated in terms of excess quantities. The same excess quantities are used in the construction of a finite-volume numerical scheme that coincides with the conservative wave propagation algorithm in the absence of phase transformation. The continuity of the excess quantities at the phase boundary leads to the conservation of genuine jumps at the phase boundary. As a result, a closed system of governing equations and jump relations can be solved numerically. Results of such calculations are presented in (Berezovski and Maugin (2002); Berezovski et al. (2002, 2003); Berezovski and Maugin (2003, 2005c); Berezovski et al. (2006, 2008)).

Straight brittle crack

Dynamic crack propagation is the subject of numerous articles and books due to its practical importance. The main difficulty in the theoretical description of the crack dynamics is the singularity of stress distribution in the vicinity of the crack tip in the framework of linear elasticity (Freund (1990); Broberg (1999); Ravi-Chandar (2004)). In practice, the singularity is avoided by means of various ways, such as the introduction of a nonlinear zone ahead of the crack tip (cohesive zone (Barenblatt (1959); Dugdale (1960)), plastic flow (Drugan et al. (1982))) or phase field models (Francfort and Marigo (1998)). The indicated models consider the velocity of the crack as given. This is, probably, the consequence of the result of the scaling analysis by Fineberg and Marder (1999) for a straight brittle crack

$$V_C = c_R \left(1 - \frac{l_0}{l} \right),$$
(32)

where V_C is the crack tip velocity, c_R is the Rayleigh wave speed, l is the length of the crack, and l_0 is the critical length. This result is coincided with that for thin plates under tension (Freund (1990)). It is concluded that the equation of motion for simple crack is correct, as long as a crack remains simple (Fineberg and Bouchbinder (2015)). However, results of numerical simulations of the crack velocity predicted by various methods can differ by three times in value (Braun and Fernández-Sáez (2014)), and all of them remain remarkable less than the Rayleigh wave speed. This means that the determination of the crack velocity is still under question even for simple cracks.

Mode I fracture in thin plate

The simplest formulation of the crack propagation problem corresponds to mode I fracture in thin plates. We consider the crack propagation in a thin cracked plate subjected to a load as shown in Figure 1.

Neglecting both geometrical and physical nonlinearities, we can write the bulk equations of linear elasticity in a homogeneous isotropic body in the absence of body
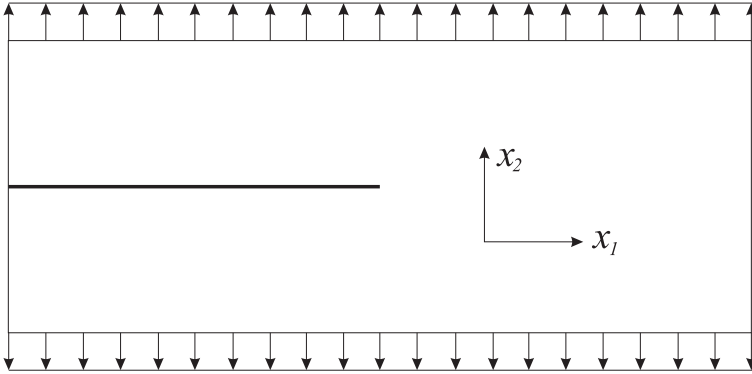
Figure 1. Model problem for a crack in a plate.

force as follows:

$$\rho_0 \frac{\partial v_i}{\partial t} = \frac{\partial \sigma_{ij}}{\partial x_j}, \tag{33}$$

$$\frac{\partial \sigma_{ij}}{\partial t} = \lambda \frac{\partial v_k}{\partial x_k} \delta_{ij} + \mu \left(\frac{\partial v_i}{\partial x_j} + \frac{\partial v_j}{\partial x_i} \right), \tag{34}$$

where t is time, x_j are spatial coordinates, v_i are components of the velocity vector, σ_{ij} is the Cauchy stress tensor, ρ_0 is the density, λ and μ are the Lamé coefficients.

In the case of thin plates, the problem can be simplified by means of the plane stress approximation (thin strip geometry, $\sigma_{i3} = 0, i = 1, 2, 3$). Corresponding solutions stress and strain fields can be found elsewhere (cf., Freund (1990); Ravi-Chandar (2004)).

For the irreversible process of crack propagation we should take into account the inequality of Clausius-Duhem

$$\frac{\partial S}{\partial t} + \frac{\partial (Q_i/\theta)}{\partial x_i} \geq 0, \tag{35}$$

where Q_i is the heat flux, S is the entropy per unit volume, and θ is temperature.

The crack front in the thin plate problem is a straight line in $x_1 - x_3$ plane, propagating in the x_1 direction. This is illustrated in Fig 2. The jump relation across crack front C corresponding to the balance of linear momentum (33) reads

$$V_C [\![\rho_0 v_i]\!] + N_j [\![\sigma_{ij}]\!] = 0. \tag{36}$$

Here V_C is the material velocity of the crack front along normal N_j.

The corresponding jump relation for the entropy should exhibit a source term

$$V_C [\![S]\!] - N_j [\![Q_j/\theta]\!] = \sigma_C \geq 0, \tag{37}$$

where σ_C is unknown scalar. The driving force and crack velocity are constrained to satisfy the second law of thermodynamics at the crack front C such that (Maugin (1997))

$$f_i V_i = \theta_C \sigma_C \geq 0. \tag{38}$$

However, the jump relations are useless until we determine the value of the velocity of the crack front.

Velocity of the crack in mode I

For given stress and strain fields we can estimate the velocity of the crack by means of the jump relation for linear momentum (36). In the small strain approximation, the material velocity V_j is connected with the physical velocity v_i by (Maugin 1993)

$$v_i = -(\delta_{ij} + \frac{\partial u_i}{\partial x_j})V_j. \tag{39}$$

Inserting the latter relation into Eq. (36), we have

$$V_C \left[\!\left[\rho_0(\delta_{ij} + \frac{\partial u_i}{\partial x_j})V_j \right]\!\right] - N_j \left[\!\left[\sigma_{ij} \right]\!\right] = 0. \tag{40}$$

The projection on the normal to the crack front reduces the last expression to

$$V_C \left[\!\left[\rho_0(1 + \varepsilon_{11})V_1 \right]\!\right] - \left[\!\left[\sigma_{11} \right]\!\right] = 0, \tag{41}$$

where σ_{11} is the component of the stress tensor normal to the crack front. Since we have no material behind the crack front, jumps are equal to values of quantities in front of the crack front which leads to

$$V_C^2 = \frac{\sigma_{11}}{\rho_0(1 + \varepsilon_{11})}. \tag{42}$$

However, we are not able to determine exact values of the stress components at the crack tip due to the square-root singularity. To be able to go further, we apply the non-equilibrium jump relation as in the case of the phase transition front
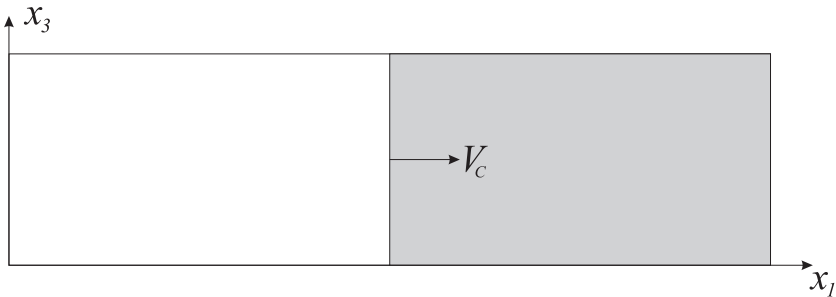
Figure 2. Crack front

(Berezovski and Maugin 2004) due to the similarity between Eq. (42) and Eq. (11)

$$\left[\!\left[\sigma_{11} + \theta \left(\frac{\partial S}{\partial \varepsilon_{11}} \right)_\sigma \right]\!\right] = 0. \tag{43}$$

It follows from Eq. (43) that the "effective" value of the normal stress at the crack front is determined by the corresponding entropy derivative

$$\sigma_{11} = -\theta \left(\frac{\partial S}{\partial \varepsilon_{11}} \right)_\sigma. \tag{44}$$

Taking into account the entropy jump at a discontinuity (Eq. (37)) and the expression for entropy production (38), we see that in the isothermal case the entropy at the crack front is dependent only on the driving force

$$S = \frac{f_C}{\theta}. \tag{45}$$

Calculating the entropy derivative on the right hand side of Eq. (44) we have

$$\sigma_{11} = -\theta \left(\frac{\partial S}{\partial \varepsilon_{11}} \right)_\sigma = \frac{f_C}{\theta} \left(\frac{\partial \theta}{\partial \varepsilon_{11}} \right)_\sigma - \left(\frac{\partial f_C}{\partial \varepsilon_{11}} \right)_\sigma. \tag{46}$$

This means that the normal stress at the crack front can be expressed in terms of the driving force as follows:

$$\sigma_{11} = f_C \frac{2(\lambda + \mu)}{\theta \alpha (3\lambda + 2\mu)} - \left(\frac{\partial f_C}{\partial \varepsilon_{11}} \right)_\sigma, \tag{47}$$

where α is the thermal expansion coefficient.

It is commonly accepted that the driving force acting at the crack tip can be calculated by means of the path-independent J-integral, which has the physical meaning of the energy release rate. The dynamic J-integral for a homogeneous cracked body (Atkinson and Eshelby (1968); Kostrov and Nikitin (1970); Freund (1972); Maugin (1994)) can be expressed in the case of mode I straight crack as follows:

$$J = \lim_{\Gamma \to 0} \int_\Gamma \left((W + K)\delta_{1j} - \sigma_{ij} \frac{\partial u_i}{\partial x_1} \right) n_j d\Gamma. \tag{48}$$

Here n_j is the unit vector normal to an arbitrary contour Γ pointing outward of the enclosed domain. The kinetic energy density, K, is given by

$$K = \frac{1}{2} \rho_0 \mathbf{v}^2. \tag{49}$$

In the two-dimensional case, the driving force is related to the value of the J-integral (48) as follows:

$$f_C = \frac{J}{a}, \tag{50}$$

where a is a scaling factor which has dimension of length.

Summing up, we can represent the "effective" stress at the crack front as

$$\sigma_{11} = \frac{AJ}{a} - \left(\frac{\partial f_C}{\partial \varepsilon_{11}}\right)_\sigma, \tag{51}$$

with

$$A = \frac{2(\lambda + \mu)}{\theta\alpha(3\lambda + 2\mu)}.$$

Simple kinetic relation

Let us check the consistency of the "effective" value of the normal stress at the crack front with existing estimations. In the simplest case, we can neglect the second term in Eq. (51), which reduces it to

$$\sigma_{11} = \frac{AJ}{a}. \tag{52}$$

In the framework of the linear theory, we can expect a linear stress-strain relation between the "effective" stress, σ_{11}, and the "effective" strain, ε_{11},

$$\sigma_{11} = B\varepsilon_{11}. \tag{53}$$

Inserting Eq. (53) into Eq. (52), we have

$$V_C^2 = \frac{\sigma_{11}}{\rho_0\left(1 + \sigma_{11}/B\right)}. \tag{54}$$

The value of the coefficient B is determined from the condition that the velocity of the crack front should approach the Rayleigh wave velocity c_R at high values of σ_{11}. In such a case, we have

$$\lim_{\sigma \to \infty} V_C^2 = c_R^2 = \frac{B}{\rho_0}. \tag{55}$$

Taking into account relations (52) and (55), we can represent Eq. (54) in the form

$$\frac{V_C^2}{c_R^2} = \left(1 + \frac{\rho_0 c_R^2 a}{AJ}\right)^{-1}. \tag{56}$$

This means that for sufficiently small values of $\rho_0 c_R^2 a/AJ$ we have in the first approximation

$$\frac{V_C^2}{c_R^2} \approx 1 - \frac{\rho_0 c_R^2 a}{AJ}. \tag{57}$$

Extracting the root from both sides of the last expression, we obtain

$$\frac{V_C}{c_R} \approx \sqrt{1 - \frac{\rho_0 c_R^2 l}{AJ}} \approx 1 - \frac{\rho_0 c_R^2 a}{2AJ}. \tag{58}$$

Actually this is another form of the well-known relation for the crack velocity (32). Thus, the "effective" value of the stress at the crack front in its simplest form does not contradict to existing estimates.

Not so simple kinetic relation

Certainly, there are other possibilities in the choice of the value of the "effective" stress at the crack front. It should be noted that Eq. (51) can be considered as the definition of averaged and excess stresses in the computational cell adjacent to the crack front in full analogy with the case of phase transitions

$$\sigma_{11} = \bar{\sigma}_{11} + \Sigma_{11}, \qquad (59)$$

with

$$\bar{\sigma}_{11} = \frac{AJ}{a}, \quad \text{and} \quad \Sigma_{11} = -\left(\frac{\partial f_C}{\partial \varepsilon_{11}}\right)_\sigma.$$

To perform calculations, we can suppose a proportionality between Σ_{11} and $\bar{\sigma}_{11}$,

$$\Sigma_{11} = D\bar{\sigma}_{11}. \qquad (60)$$

In such a case, we have the following expression for the velocity of the crack front

$$V_C^2 = \frac{\bar{\sigma}_{11}(1+D)}{\rho_0\left(1+\bar{\sigma}_{11}/B\right)}. \qquad (61)$$

Consequently,

$$\lim_{\sigma \to \infty} V_C^2 = \frac{B}{\rho_0}\left(1 + \lim_{\sigma \to \infty}\frac{\Sigma_{11}}{\bar{\sigma}_{11}}\right) = c_R^2\left(1+D\right). \qquad (62)$$

As one can see, here the limiting value of the velocity of the crack front is different from the value of the Rayleigh wave velocity. Denoting the limiting value of the velocity of the crack front as V_T, we can represent the expression for the velocity of the crack front as follows:

$$V_C^2 = V_T^2\left(1 + \frac{\rho_0 c_R^2 a}{AJ}\right)^{-1} = V_T^2\left(1 - \left(1 + \frac{AJ}{\rho_0 c_R^2 a}\right)^{-1}\right). \qquad (63)$$

To be able to compare the obtained relation with experimental data, we note that the value of the J-integral is proportional to the square of the stress intensity factor K_I in the considered problem. Therefore, we can rewrite the last expression in terms of the stress intensity factor

$$V_C^2 = V_T^2\left(1 + \frac{Ma}{K_I^2}\right)^{-1} = V_T^2\left(1 - \left(1 + \frac{K_I^2}{Ma}\right)^{-1}\right), \qquad (64)$$

where the coefficient M depends on properties of the material.

Thus, the derived kinetic relation contains two model parameters: the limiting velocity V_T, which directly corresponds to the condition taken for the excess stress at the crack front, and the characteristic length scale a. Both model parameters may by adjusted to fit experimental data.

It should be noted that the expression (64) is applied only for the values $K_I > K_{Ic}$, where K_{Ic} is the critical value of the stress intensity factor (fracture toughness). The 'averaged' $K_I - V_C$ relationship suggested by Ravi-Chandar (2004) is based on the experimental observations (Ravi-Chandar and Knauss (1984)), where the crack velocity remained constant in each individual experiment. It is easy to see that for sufficiently small values of ML in Eq. (64), we will have a practically constant crack velocity. Its limiting value V_T appears to be dependent on the conditions of experiment.

One can suppose that the characteristic length a may be taken to be similar to the process zone length

$$a \sim \frac{K_{Ic}^2}{\sigma_*^2}. \tag{65}$$

In the thin strip geometry, it is possible to relate the values of σ_* and J (Hauch and Marder (1998)), which leads to

$$a \sim \frac{K_{Ic}^2}{J}. \tag{66}$$

In this case we arrive at an expression for the velocity of the crack front in the form

$$V_C^2 = V_T^2 \left(1 + \frac{M' K_{Ic}^2}{K_I^4} \right)^{-1} = V_T^2 \left(1 - \left(1 + \frac{K_I^4}{M' K_{Ic}^2} \right)^{-1} \right), \tag{67}$$

where M' is another material constant.

As the comparison of theoretical relations (Eqs. (64) and (67)) with experimental data shows (Berezovski and Maugin (2007a, 2010)), a good fit of the experimental curves is obtained by adjusting values of the limiting velocity and of the characteristic length.

Conclusions

The prediction of the location of a propagating discontinuity is important from both theoretical and practical points of view. Theoretically, the existence of a propagating discontinuity leads to an incompleteness of the continual description expressed in the indeterminacy of the velocity of such a discontinuity. In practice, this indeterminacy results in the necessity of an additional experimental work.

As it is shown in the paper, the indeterminacy of the velocity of a propagating phase-transition front can be avoided in computations implementing the conservation of the genuine jump at the phase boundary, at least in the simple one-dimensional situation. In principle, the kinetic relation can be extracted from this condition under suitable assumptions (Berezovski and Maugin (2005b, 2010)).

Computation of the crack tip velocity needs, however, the knowledge of the kinetic relation in advance (because of the singularity at the crack tip). Proposed kinetic relations are still dependent on experimentally determined material parameters, but with the reduced corresponding work.

References

Abeyaratne R and Knowles JK (1990) On the driving traction acting on a surface of strain discontinuity in a continuum. *Journal of the Mechanics and Physics of Solids* 38(3): 345–360.

Abeyaratne R and Knowles JK (2006) *Evolution of Phase Transitions: A Continuum Theory*. Cambridge University Press.

Ani W and Maugin GA (1988) One-dimensional nonlinear motions in electroelastic solids: Characteristics and shock waves. *Zeitschrift für angewandte Mathematik und Physik ZAMP* 39(3): 277–298.

Ani W and Maugin GA (1989) Basic equations for shocks in nonlinear electroelastic materials. *The Journal of the Acoustical Society of America* 85(2): 599–610.

Atkinson C and Eshelby J (1968) The flow of energy into the tip of a moving crack. *International Journal of Fracture Mechanics* 4(1): 3–8.

Barenblatt G (1959) Concerning equilibrium cracks forming during brittle fracture. the stability of isolated cracks. relationships with energetic theories. *Journal of Applied Mathematics and Mechanics* 23(5): 1273–1282.

Berezovski A, Engelbrecht J and Maugin GA (2002) A thermodynamic approach to modeling of stress-induced phase-transition front propagation in solids. In: *IUTAM Symposium on Mechanics of Martensitic Phase Transformation in Solids*. Springer, pp. 19–26.

Berezovski A, Engelbrecht J and Maugin GA (2003) Numerical simulation of thermoelastic wave and phase-transition front propagation. In: *Mathematical and Numerical Aspects of Wave Propagation WAVES 2003*. Springer, pp. 759–764.

Berezovski A, Engelbrecht J and Maugin GA (2006) Modeling and numerical simulation of nonclassical effects of waves, including phase transition front. In: *Universality of Nonclassical Nonlinearity*. Springer, pp. 203–219.

Berezovski A, Engelbrecht J and Maugin GA (2007) Front dynamics in inhomogeneous solids. *Proceedings of Estonian Academy of Sciences, Ser. Physics, Mathematics* 56(2): 155–161.

Berezovski A, Engelbrecht J and Maugin GA (2008) *Numerical simulation of waves and fronts in inhomogeneous solids.* World Scientific Singapore.

Berezovski A and Maugin GA (2002) Thermoelastic wave and front propagation. *Journal of Thermal Stresses* 25(8): 719–743.

Berezovski A and Maugin GA (2003) Simulation of wave and front propagation in elastic and thermoelastic heterogeneous materials. *Computational Materials Science* 28(3): 478–485.

Berezovski A and Maugin GA (2004) On the thermodynamic conditions at moving phase-transition fronts in thermoelastic solids. *Journal of Non-Equilibrium Thermodynamics* 29(1): 37–51.

Berezovski A and Maugin GA (2005a) Driving force in simulation of phase transition front propagation. In: *Mechanics of Material Forces*. Springer, pp. 289–297.

Berezovski A and Maugin GA (2005b) On the velocity of a moving phase boundary in solids. *Acta Mechanica* 179(3-4): 187–196.

Berezovski A and Maugin GA (2005c) Stress-induced phase-transition front propagation in thermoelastic solids. *European Journal of Mechanics-A/Solids* 24(1): 1–21.

Berezovski A and Maugin GA (2007a) Moving singularities in thermoelastic solids. *International Journal of Fracture* 147(1-4): 191–198.

Berezovski A and Maugin GA (2007b) On the propagation velocity of a straight brittle crack. *International Journal of Fracture* 143(2): 135–142.

Berezovski A and Maugin GA (2010) Jump conditions and kinetic relations at moving discontinuities. *ZAMM-Journal of Applied Mathematics and Mechanics/Zeitschrift für Angewandte Mathematik und Mechanik* 90(7-8): 537–543.

Braun M and Fernández-Sáez J (2014) A new 2d discrete model applied to dynamic crack propagation in brittle materials. *International Journal of Solids and Structures* 51(21): 3787–3797.

Broberg KB (1999) *Cracks and Fracture*. Academic Press.

Christian JW (1965) *The Theory of Transformations in Metals and Alloys*. Pergamon, London.

Daher N and Maugin GA (1986) The method of virtual power in continuum mechanics application to media presenting singular surfaces and interfaces. *Acta Mechanica* 60(3-4): 217–240.

Dascalu C and Maugin G (1994) Energy-release rates and path-independent integrals in electroelastic crack propagation. *International Journal of Engineering Science* 32(5): 755–765.

Dascalu C and Maugin GA (1993) Material forces and energy-release rates in homogeneous elastic bodies with defects. *Comptes Rendus De L Academie Des Sciences Serie li* 317(9): 1135–1140.

Dascalu C and Maugin GA (1995) On the dynamic fracture of piezoelectric materials. *The Quarterly Journal of Mechanics and Applied Mathematics* 48(2): 237–255.

Drugan W, Rice J and Sham T (1982) Asymptotic analysis of growing plane strain tensile cracks in elastic-ideally plastic solids. *Journal of the Mechanics and Physics of Solids* 30(6): 447–473.

Dugdale DS (1960) Yielding of steel sheets containing slits. *Journal of the Mechanics and Physics of Solids* 8(2): 100–104.

Fineberg J and Bouchbinder E (2015) Recent developments in dynamic fracture: some perspectives. *International Journal of Fracture* 196(1-2): 33–57.

Fineberg J and Marder M (1999) Instability in dynamic fracture. *Physics Reports* 313(1): 1–108.

Fomethe A and Maugin GA (1997) Propagation criterion for phase-transition fronts in thermoelastic ferromagnets. *Proceedings of Estonian Academy of Sciences, Ser. Physics, Mathematics* 46: 48–54.

Fomethe A and Maugin GA (1998) On the crack mechanics of hard ferromagnets. *International Journal of Non-Linear Mechanics* 33(1): 85–95.

Francfort GA and Marigo JJ (1998) Revisiting brittle fracture as an energy minimization problem. *Journal of the Mechanics and Physics of Solids* 46(8): 1319–1342.

Freund L (1972) Energy flux into the tip of an extending crack in an elastic solid. *Journal of Elasticity* 2(4): 341–349.

Freund LB (1990) *Dynamic Fracture Mechanics*. Cambridge university press.

Gurtin ME (2000) *Configurational Forces as Basic Concepts of Continuum Physics*. Springer.

Hauch J and Marder M (1998) Energy balance in dynamic fracture, investigated by a potential drop technique. *International Journal of Fracture* 90(1-2): 133–151.

Heidug W and Lehner F (1985) Thermodynamics of coherent phase transformations in nonhydrostatically stressed solids. *Pure and Applied Geophysics* 123(1): 91–98.

Kienzler R and Herrmann G (2000) *Mechanics in Material Space: With Applications to Defect and Fracture Mechanics*. Springer.

Kostrov B and Nikitin L (1970) Some general problems of mechanics of brittle fracture (Brittle fracture mechanism models and connection with rheological properties of material, deriving relations for Griffith energy criterion). *Archiwum Mechaniki Stosowanej* 22(6): 749–776.

Maugin GA (1993) *Material Inhomogeneities in Elasticity*. CRC Press.

Maugin GA (1994) On the J-integral and energy-release rates in dynamical fracture. *Acta Mechanica* 105(1-4): 33–47.

Maugin GA (1995) Material forces: concepts and applications. *Applied Mechanics Reviews* 48(5): 213–245.

Maugin GA (1997) Thermomechanics of inhomogeneous-heterogeheous systems: application to the irreversible progress of two- and three-dimensional defects. *ARI-An International Journal for Physical and Engineering Sciences* 50: 41–56.

Maugin GA (1998) On shock waves and phase-transition fronts in continua. *ARI-An International Journal for Physical and Engineering Sciences* 50(3): 141–150.

Maugin GA (2000) On the universality of the thermomechanics of forces driving singular sets. *Archive of Applied Mechanics* 70(1-3): 31–45.

Maugin GA (2003) Pseudo-plasticity and pseudo-inhomogeneity effects in materials mechanics. *Journal of Elasticity* 71(1-3): 81–103.

Maugin GA (2011) *Configurational Forces: Thermomechanics, Physics, Mathematics, and Numerics*. CRC Press.

Maugin GA and Berezovski A (1999) Material formulation of finite-strain thermoelasticity and applications. *Journal of Thermal Stresses* 22(4-5): 421–449.

Maugin GA and Berezovski A (2003) Recent progress in the numerical simulation of the thermoelastodynamics of phase-transition fronts. In: *Proceedings of the 5th International Congress on Thermal Stresses and Related Topics*. Virginia Tech, Blacksburg, pp. KNL–3–1– KNL–3–6.

Maugin GA and Berezovski A (2008) Introduction to the thermomechanics of configurational forces. *Atti della Accademia Peloritana dei Pericolanti-Classe di Scienze Fisiche, Matematiche e Naturali* 86(S1): 1–16.

Maugin GA and Berezovski A (2009) On the propagation of singular surfaces in thermoelasticity. *Journal of Thermal Stresses* 32(6-7): 557–592.

Maugin GA and Trimarco C (1992) Pseudomomentum and material forces in nonlinear elasticity: variational formulations and application to brittle fracture. *Acta Mechanica* 94(1-2): 1–28.

Maugin GA and Trimarco C (1995a) Configurational forces and coherent phase-transition fronts in thermoelastic solids. In: *IUTAM Symposium on Anisotropy, Inhomogeneity and Nonlinearity in Solid Mechanics*. Springer, pp. 345–350.

Maugin GA and Trimarco C (1995b) The dynamics of configurational forces at phase-transition fronts. *Meccanica* 30(5): 605–619.

Maugin GA and Trimarco C (1997) Driving force on phase transition fronts in thermoelectroelastic crystals. *Mathematics and Mechanics of Solids* 2(2): 199–214.

Maugin GA and Trimarco C (2001) Elements of field theory in inhomogeneous and defective materials. In: *Configurational Mechanics of Materials*. Springer, pp. 55–128.

Ravi-Chandar K (2004) *Dynamic Fracture*. Elsevier.

Ravi-Chandar K and Knauss W (1984) An experimental investigation into dynamic fracture: III. On steady-state crack propagation and crack branching. *International Journal of Fracture* 26(2): 141–154.

Sabir M and Maugin GA (1996) On the fracture of paramagnets and soft ferromagnets. *International Journal of Non-Linear Mechanics* 31(4): 425–440.

Shaw JA and Kyriakides S (1997) On the nucleation and propagation of phase transformation fronts in a NiTi alloy. *Acta Materialia* 45(2): 683–700.

Truskinovsky L (1987) Dynamics of non-equilibrium phase boundaries in a heat conducting non-linearly elastic medium. *Journal of Applied Mathematics and Mechanics* 51(6): 777–784.